Hindawi
Advances in Materials Science and Engineering
Volume 2022, Article ID 7323588, 8 pages
https://doi.org/10.1155/2022/7323588

Research Article

Experimental Investigation on Reactive Orange 16 Removal Using Waste Biomass of *Ulva prolifera*

Gokulan Ravindiran,[1] **Kalyani Gaddam**,[2] **and Killi Sunil**[3]

[1]*Department of Civil Engineering, GMR Institute of Technology, Rajam 532 127, Andhra Pradesh, India*
[2]*Department of Civil Engineering, Nadimpalli Satyanarayana Raju Institute of Technology, Visakhapatnam 531173, Andhra Pradesh, India*
[3]*Department of Chemical Engineering, College of Engineering and Technology, Samara University, Afar, Ethiopia*

Correspondence should be addressed to Killi Sunil; sunilkilli@su.edu.et

Received 23 April 2022; Accepted 6 May 2022; Published 23 May 2022

Academic Editor: Samson Jerold Samuel Chelladurai

Copyright © 2022 Gokulan Ravindiran et al. This is an open access article distributed under the Creative Commons Attribution License, which permits unrestricted use, distribution, and reproduction in any medium, provided the original work is properly cited.

Ulva prolifera marine seaweed was tested for its capacity to eliminate reactive orange 16 (RO16) from aqueous solutions. Algae has recently been regarded as one of the most environmental friendly wastewater treatment methods and resources. The batch study used variations in solution pH, sorbent dosage, initial dye concentration, and temperature. The biochar was characterized using Fourier transform infrared (FT-IR) spectroscopy, an elemental analyser, proximate analysis, and a BET analyser. The adsorption mechanism was further investigated using adsorption isotherm and kinetic models. The thermodynamic analysis was performed by varying temperatures at different dye concentrations and calculating thermodynamic parameters such as Gibbs free energy, enthalpy, and entropy. The study was performed to evaluate the sorbent's performance in real-time wastewater treatment, a variety of chemicals, solid-liquid ratios, and regeneration cycles that were used to determine desorption efficiency.

1. Introduction

Dyes are a type of harmful contaminant that has been widely used for a variety of purposes. Paint, paper and pulp, textiles, and plastic sectors all used dyes. Natural and synthetic dyes are the two types of dyes [1]. Natural dyes have a low environmental impact; however, due to the dye availability and demand, synthetic dyes have become more popular. Water stability, binding nature, water fastness, and the development of strong chemical connections between fabric and dye molecules are all properties of synthetic dyes [2]. There are various benefits, including low cost, a variety of hues, and improved qualities of dyed materials. Acid dyes, basic dyes, reactive dyes, direct dyes, disperse dyes, and sulphur dyes are all types of synthetic dyes. Dyes are carcinogenic and nonbiodegradable in general [3]. Dye molecules penetrate the human ecosystem's food chain, causing a variety of health problems. Cancer, kidney failure, lung problems, liver damage, and skin disease are just a few of the devastating conditions that can arise. Due to their improved properties, reactive dyes are the most commonly used dyes.

Reactive dyes are used to print cellulose materials and come in a wide range of hues [4]. According to estimates, around 30% of the dyes used in the printing industry are reactive dyes. Reactive dyes form strong chemical links (covalent bonds) between the fabric and the dye, making it difficult to remove. The presence of aromatic ring structures inside reactive dyes causes this. Furthermore, wastewater from reactive dyeing industries is extremely alkaline, with a pH of more than 10 to 11 [5]. Reactive dyes require sodium carbonate or soda ash for dyeing, and this wastewater is used to wash nearly 10% to 20% of the colours. In the dyeing process, sodium alginate is utilised as a thickener. These alkaline solvents pollute wastewater more and have negative environmental consequences [6].

Membrane filtration, ion exchange, sedimentation, electrocoagulation, reverse osmosis, and phytoremediation are some of the most often utilised treatment methods [7].

However, the biggest disadvantage of these treatment options is the treatment cost and time involved. Adsorption is regarded as one of the most often utilised processes in the dyeing industry. As a biosorbent, a variety of naturally occurring materials such as natural clay, hydrated silicates, zeolites, waste biomass, sewage sludge, seaweeds, and natural seeds are used [8]. One of the most widely used sorbents in the dye removal procedure is activated carbon. The cost of producing activated carbon is extremely high, so finding alternative low-cost sorbents has become a must-do research project [9].

Biochar is a carbon-enhanced substance created in a low-oxygen environment from waste biomass. The pyrolysis, gasification, hydrothermal carbonization, and torrefaction processes were used to create biochar. Pyrolysis was regarded as one of the most widely utilised ways of producing biochar due to its several advantages [10]. In the pyrolysis process, the heating rate and residence time may be easily regulated. Slow, quick, flash, and microwave-assisted pyrolysis are the other types of pyrolysis. Slow pyrolysis is the most common pyrolysis method, and it is utilised to make charcoal on a big scale [11]. The current study investigated the potential of *Ulva prolifera* biomass for biochar production and assessed the removal efficiency of reactive orange 16 in a batch process. *Ulva prolifera* was abundant in the South Tamil Nadu region of India's east coast, but its application was restricted. Waste biomass may be harvested at a minimal cost, and it may be processed into an environmentally friendly product. *Ulva prolifera* contains a polysaccharide called group *Ulva*, which contains carbonyl, carboxyl, amine, and amino groups. These functional groups will improve sorption capacity and reduce pollutant levels.

2. Materials and Methods

2.1. Seaweed Collection and Chemicals. *Ulva prolifera* was found in the South Tamil Nadu region of India's east coast. In the laboratory, the needed amount of biomass was gathered. The biomass was cleaned with deionized water after being washed with tap water. The biomass was rinsed and dried for 24 hours. Using a shredder, the dry biomass was shredded to 7.5 mm and then heated at 103 °C for 24 hours to eliminate the moisture content. The dried biomass was then used in a muffle furnace to produce biochar. To ensure lack of oxygen, the muffle furnace was first cleaned with nitrogen gas. The crucible was filled with the necessary amount of biomass and was covered with aluminum foil with two small openings. The biochar was made using a varied pyrolysis temperature range of 300–500 °C [12].

2.2. Biochar Characterization. An elemental analyser was used to determine the carbon, hydrogen, nitrogen, oxygen, and sulphur content of the biochar. The functional groups present in the biochar were determined using Fourier-transform infrared spectroscopy. The BET analyser was used to determine the specific surface area, pore volume, and average pore size of the biochar in order to assess its physical qualities. Furthermore, point of zero charge studies was carried out to identify the pH at which the surface is neutral in order to have a better understanding of the sorption mechanism.

2.3. Dye Batch Adsorption Studies. Batch adsorption experiments were carried out in the same way as in our previous studies [12]. As described in our previous investigations, adsorption isotherms, kinetic studies, thermodynamic studies, and regeneration experiments were all used to better understand the sorption process of biochar [12].

3. Results and Discussion

3.1. Biochar Characterization. The basic profile of *U. prolifera*-derived biochar at various pyrolysis temperatures is presented in Table 1. It was obvious from the results that the carbon content did not change significantly as the pyrolysis temperature varied. However, when the pyrolysis temperature rose, the hydrogen, oxygen, nitrogen, and sulphur content of the biochar dropped. The H/C ratio declined as the temperature rose, demonstrating that the biochar's aromaticity is lower at lower temperatures than at higher pyrolysis temperatures. The O/C ratio drops as pyrolysis progresses, indicating increased hydrophobicity and carbonization degree. With increased pyrolysis, the polarity index $((O + N)/C)$ declined, indicating a decrease in O-containing functional groups. As a result, it was determined that a pyrolysis temperature of 350 °C was the best temperature for improving biochar characteristics [13]. Furthermore, the point of zero charges played an important role in harmful pollutant sorption. The point of zero charges was calculated to determine the surface charge of the biochar. Table 1 shows that when the pyrolysis temperature rises, the point of zero charges rises as well. Biochar acquires negative charges at higher temperatures and favours cationic colours, whereas at lower temperatures, biochar acquires more positive charges and may favour anionic dyes [14]. The current study looks at the reactive ions that are negatively charged and have an acidic character, which is essential for maximum sorption. At a pyrolysis temperature of 350°C, the BET surface area was measured. The average pore size was 5.66 nm, with a specific surface area of 125.53 m2/g and total pore volume of 0.182 cm3/g. According to the BET analysis, biochar has a large surface area that favours dye molecule sorption to the greatest extent possible.

FT-IR spectra of the raw biochar and RO16 dye bounded biochar are summarized in Table 2. The results show that there was a significant shift in the spectra following the sorption of RO16 dye molecules. This may have been changed because the sulfonate groups in the dye molecules affected the functional groups on the biochar's surface [15].

3.2. Dosage of Biochar on RO16 Adsorption. The role of adsorbent dosage in the removal of RO16 is depicted in Figure 1. It was clear from the results that increasing the dose increased efficiency while decreasing absorption capacity.

Table 1: Biochar's elemental profile at various pyrolysis temperatures.

Temperature (°C)	C (%)	N (%)	O (%)	H (%)	S (%)	H/C	O/C	(O + N)/C	pH_{pzc}
300	60.52	4.44	22.24	3.98	8.82	0.07	0.37	0.44	6.22
350	63.07	4.52	19.72	3.73	8.96	0.06	0.31	0.38	6.68
400	64.52	4.69	18.75	2.8	9.24	0.04	0.29	0.36	7.35
450	60.64	3.48	17.86	1.8	16.22	0.03	0.29	0.35	10.2
500	60.63	2.84	14.66	1.2	20.67	0.02	0.24	0.29	10.5

C: carbon; H: hydrogen; S: sulphur; O: oxygen; N: nitrogen.

Table 2: FT-IR spectra (before and after sorption).

Spectral groups	Raw biochar	RO16 dye bounded biochar
O-H in the carboxyl	3507	3496
C-H stretching bands	2825	2910
Aromatic C=C or C=O	1717	1725
Stretches of $C-H_2$	1537	1505
Aliphatic C-O-C	1239	1298
Aromatic C-H	895	815

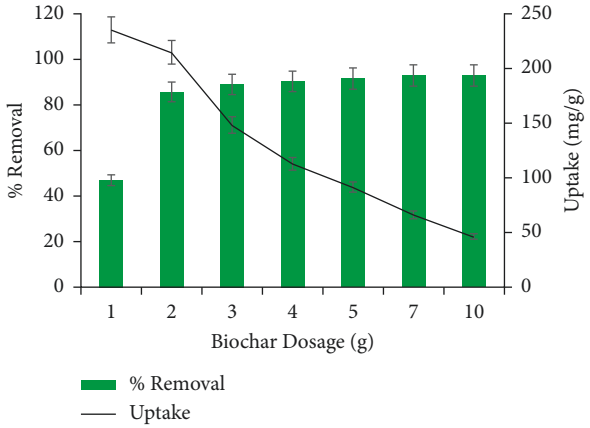


Figure 1: The effect of biochar concentration on RO16.

When the dose was increased from 1 to 10 g/L, for example, the elimination efficiency improved from 47 to 93 percent, whereas the absorption capacity reduced from 235 to 46.6 mg/g. The availability of binding sites to adsorb dye molecules was very high at larger dosages, and vice versa. Due to extra dye molecules that may boost the sorption capacity of the biochar, the binding sites were entirely occupied with the dye molecules at a lower dose [16]. It was obvious from the results that biochar had a significant binding affinity for dye molecules, even at low doses. For subsequent batch studies, a biochar dose of 2 g/L was recommended based on both the removal efficiency and adsorption capacity.

3.3. Adsorption of RO16 and the Effect of Equilibrium pH. The role of solution pH on RO16 sorption is demonstrated in Figure 2. The batch findings revealed that increasing the pH reduced the removal effectiveness of RO16 dye molecules as well as the biochar's sorption capacity. When pH of the solution was increased from 1.75 to 5, for example, the

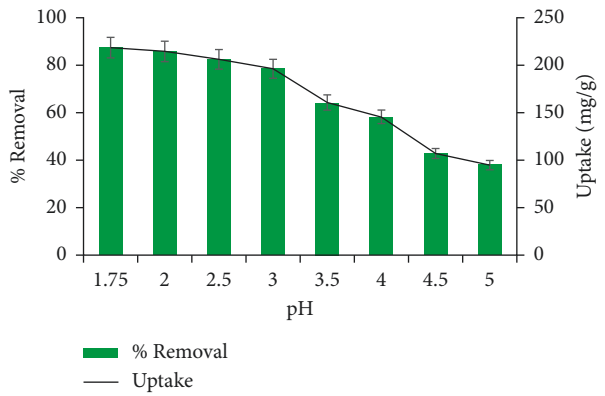


Figure 2: The effect of pH on the elimination of RO16.

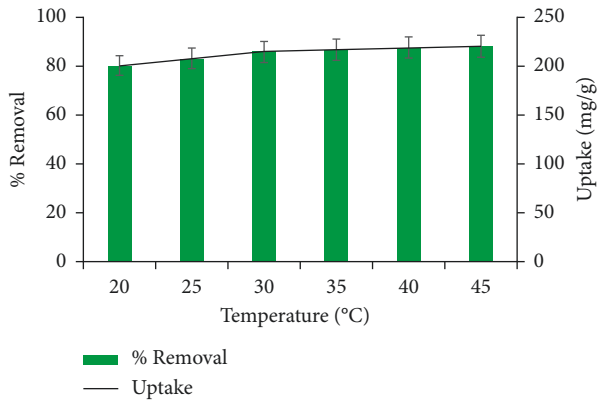


Figure 3: Temperature effects on RO16 removal.

removal efficiency dropped from 87.4 to 38 percent. The point of zero charge (pHpzc) of *U. prolifera*-derived biochar can be linked to this result. The pHpzc of biochar made from *U. prolifera* was found to be 6.68. This means that the biochar is neutral at a pH of 6.68. A stronger positive charge will emerge over the surface of the biochar if pH is reduced from 6.68, whereas a negative charge will grow over the surface of the biochar if pH is increased above 6.68. As a result, at a pH of 1.75, maximal positive ions will be present on the surface of the biochar, and reactive dyes with negative charged ions are known as anionic dyes. As a result, the biochar and the reactive dyes' negative ions will attract each other electrostatically [17]. An increase in pH, on the other hand, will result in a decrease in positive ions and electrostatic repulsion between biochar and dye molecules. As a result, it was determined that pHpzc enhanced dye molecule sorption.

Table 3: Adsorption isotherm model constants.

Model	Constants	Values	Model	Constants	Values
		Two-parameter model			
Freundlich	K_F	32.24	Langmuir	Q_0	98.92
	$1/n_F$	0.39		b	0.3254
	R^2	0.8248		R^2	0.9264
		Three-parameter model			
Redlich–Peterson	K_{RP}	9.3521	Vieth–Sladek	Q_{MVS}	374.49
	α_{RP}	0.0205		B_{VS}	0.0259
	β_{RP}	1.0786		N_{VS}	1.1061
	R^2	0.9694		R^2	0.9555
Sips	K_S	4.4667	Radke–Prausnitz	Q_{MRP}	374.52
	β_S	1.3691		K_{RP}	0.0259
	a_S	0.0168		n_{RP}	1.1061
	R^2	0.9730		R^2	0.9691
Toth	Q_{max}	268.11	Fritz–Schlunder – III	Q_{MFS}	0.0205
	b_T	0.0317		K_{FS}	454.30
	n_T	0.7066		N_{FS}	1.0786
	R^2	0.9703		R^2	0.9557
Hill	q_{mH}	259.23	Unilin	Q_{MU}	0.0199
	n_H	1.4520		A_U	466.83
	K_H	69.1832		B_U	1.0842
	R^2	0.9729		R_2	0.9694
Khan	Q_{max}	344.77			
	Bk	0.027			
	Ak	1.0841			
	R^2	0.9694			

3.4. Temperature Effects on RO16 Adsorption. Temperature is an important criterion for determining the extent of adsorption on the sorbent. Adsorption can occur as a result of either physical or chemical adsorption. For any sorbent and harmful contaminants, determining the adsorption mechanism is critical. When the rate of sorption capacity of the sorbent decreases as the temperature rises, the adsorption may be classified as physical adsorption. The kinetic energy of dye molecules increase as the temperature rises, causing them to escape from the surface of the biochar and reducing sorption [18]. Chemical adsorption increases as temperature rises, as rising temperatures result in the creation of strong interactions between dye molecules and biochar to the greatest extent possible. When dye molecules occupy homogenous monolayer adsorption throughout the surface of the sorbent to their maximal extent, temperature causes a drop in adsorption [19]. When multilayer adsorption begins, temperature causes a decrease in adsorption. The effect of temperature on the sorption process is depicted in Figure 3. The removal efficiency increased from 80.2 to 88 percent when the temperature was raised from 20 to 45 °C. It was obvious from the results that adsorption was due to chemical adsorption, and that it also indicated endothermic processes, which occur spontaneously at higher temperatures.

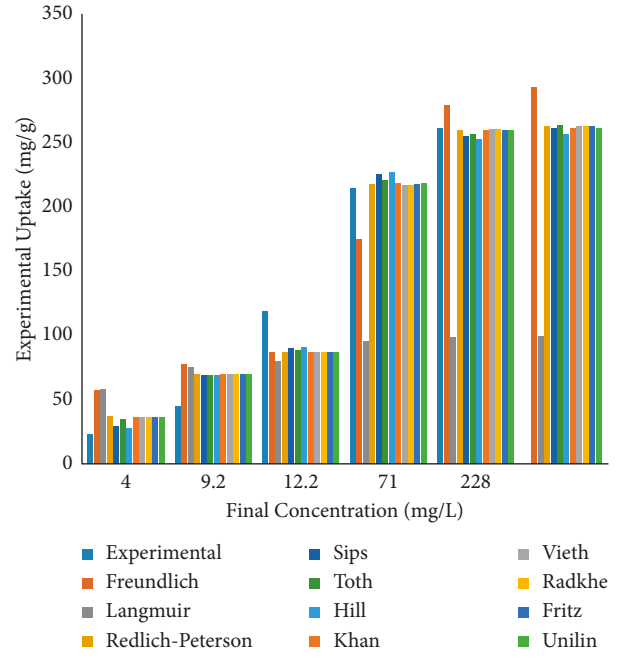


Figure 4: Dye sorption isotherms on RO16 removal using *Ulva prolifera*-derived biochar.

3.5. Isotherm and Kinetics. Adsorption mechanisms can be determined using adsorption isotherm models in addition to the sorption of any harmful contaminants. Using multiple two- and three-parameter isotherm models, the current study predicted the sorbent's absorption capacity. The model constants of various isotherm models are listed in Table 3. For the Radke–Prausnitz isotherm model, the maximum estimated sorption was 374.2 mg/g. Other models anticipated that the sorbent would have a very high sorption capacity. The anticipated sorption for Vieth–Sladek, Toth, Hill, and Khan isotherm models, for example, was 374.49,

Table 4: PFO and PSO kinetic model constants.

Dyes	Model constants	Model constants	100 mg/L	250 mg/L	500 mg/L	750 mg/L	1000 mg/L
RO16	PFO	Q_e	44.40	116.17	214.81	256.83	256.75
		k_1	0.0569	0.0530	0.0429	0.0425	0.0526
		R^2	0.9892	0.9953	0.9989	0.9952	0.9920
	PSO	Q_e	47.85	125.74	235.21	281.13	278.24
		k_2	0.0020	0.0007	0.0003	0.0002	0.0003
		R^2	0.9958	0.9963	0.9993	0.9967	0.9956

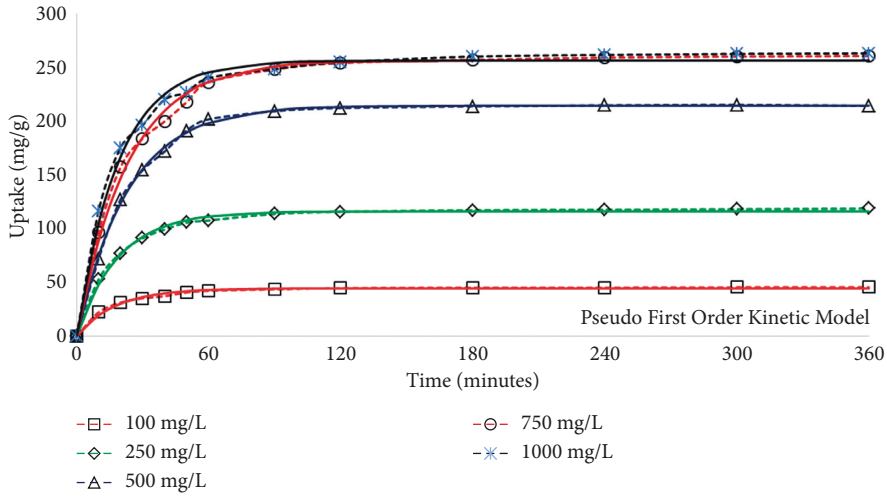


Figure 5: Observations on the elimination of RO16 using the PFO kinetic model.

268.11, 259.23, and 344.77 mg/g. These results show that biochar has a high sorption capacity for RO16 dye molecules. At constant temperature or pressure, an adsorption isotherm is utilised to forecast the fluctuation in adsorbate quantity on the adsorbent [20]. The Freundlich isotherm's correlation coefficient was quite low, 0.8248, indicating that the experiment's results were not in excellent agreement with the model's projected results. If the adsorption involves physisorption, the Freundlich isotherm model often fits; therefore, sorption of RO16 may follow chemisorption. Table 3 shows that the predictions of the Langmuir isotherm model outperform those of the Freundlich model. Langmuir was found to have a correlation coefficient of 0.9265, which explains the adsorption mechanism. The isotherm result suggests that adsorption sites will be uniformly available on the surface of the biochar, that each binding site in the biochar will bind only one dye molecule (monolayer adsorption), and that dynamic equilibrium conditions would exist between the adsorbate and the adsorbent [21]. Figure 4 depicts the expected sorption of several isotherm models.

3.6. Kinetic Studies. The amount of adsorbate adsorbed to the adsorbent at a constant concentration at changing time intervals is determined using adsorption kinetics. The varied model constants of the PFO and PSO kinetic models are presented in Table 4. Figures 5 and 6 show the absorption of different concentrations at various time periods. It was obvious from the data that the PSO kinetic model had the highest correlation coefficient. According to PSO kinetic models, the amount of adsorbate adsorbed to the adsorbent is exactly proportional to the accessible binding sites on the sorbent [22]. This also confirms that the dye molecules were absorbed through chemisorption. The data also show that the dye molecules absorbed the most for the first 60 minutes, and increasing the period resulted in relatively minimal dye molecule sorption. Initially, about 90% of the solution was completed in 60 minutes. As a result, for future batch experiments, a 120-minute equilibrium time may be explored.

3.7. Thermodynamic Studies. Batch tests were conducted at temperatures ranging from 298 to 323 K, pH of 2, biochar dose of 2 g/L, and starting concentrations ranging from 100–1000 mg/L to determine the thermodynamic parameters. The various thermodynamic characteristics under various operating circumstances are reported in Table 5 [23]. It was determined from the batch temperature results that sorption enhanced with increasing temperature, indicating an endothermic process. The intraparticle diffusion will be aided by increasing the temperature, which will result in additional binding sites for the sorption. This could help colour molecules bind to each other at higher temperatures. The thermodynamic parameter, which follows the law of thermodynamics, will provide more insight on the nature of processes. Table 5 shows that, as the temperature rises from 298 to 323 K, the ΔG^o value rises as well, and it becomes negative. The values of ΔH^o and ΔS^o were also found to be positive. It was obvious from the results that the sorption mechanism is governed by the constraints $\Delta G^o > 0$, $\Delta H^o > 0$,

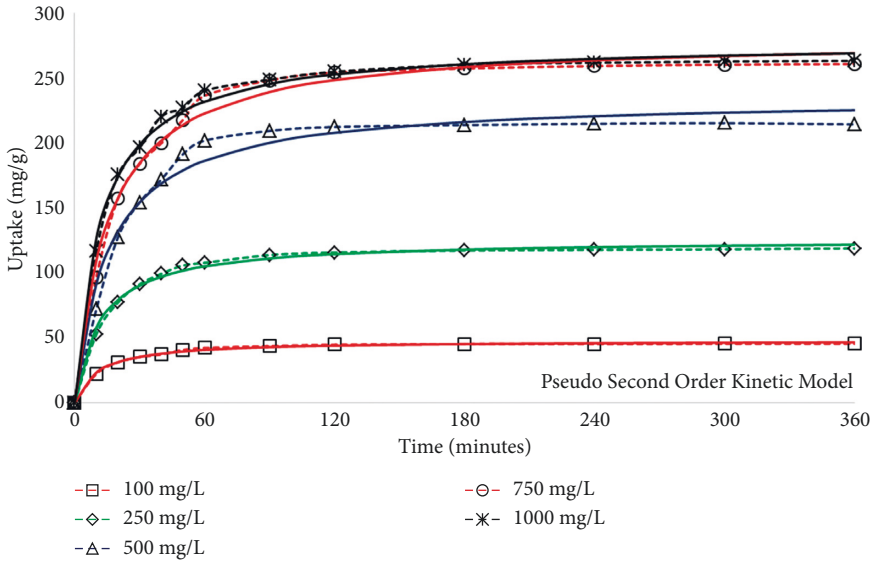


Figure 6: Observations on the elimination of RO16 using the PSO kinetic model.

Table 5: Thermodynamic parameters for the sorption of RO16.

Dye	Temperature (K)	K_L (L/mol)	ΔG° (kJ/mol)	ΔH° (kJ/mol)	ΔS° (kJ/mol/K)
RO16	298	4.76	−3.87	129.18	0.3896
	303	10.36	−5.89		
	308	34.73	−9.09		
	313	66.90	−10.94		
	318	165.42	−13.51		
	323	222.00	−14.51		

and $\Delta S^o > 0$. These conditions suggest that adsorption occurs spontaneously at high temperatures, that reactions are endothermic, and that there are a lot of randomness at the solid-liquid interface [23]. The spontaneous nature of sorption shows that dye molecules bind to one other without the need of any external forces. The sorption process can happen quickly or slowly, and it is unrelated to reaction rates or kinetics. This spontaneous nature also suggests that the reaction will proceed in a forward direction, possibly resulting in the formation of more products. It is also determined that the S^o is very low (0.3896 kJ/mol/K), implying that the sorbent's structural composition may have changed significantly [23]. Because the ΔH^o value was more than 80 kJ/mol, it was also inferred that the sorption process followed chemisorption. Figure 7 illustrates the Van't Hoff plot of RO16 onto *U. prolifera*-derived biochar.

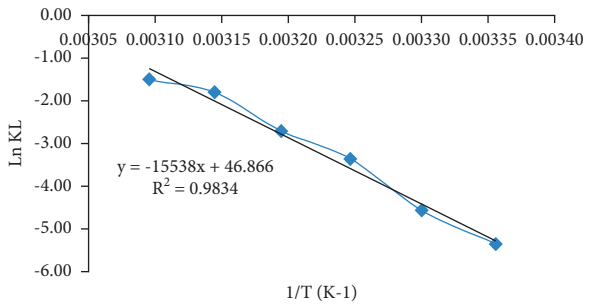


Figure 7: Van't Hoff plot of RO16 onto *U. prolifera*-derived biochar.

3.8. Regeneration Studies. The adsorption process is reversed in the desorption process. Thermal regeneration and solvent regeneration can both be used to regenerate spent biochar. When compared to the thermal regeneration technique, several researchers believe that solvent regeneration is the preferred option. Inorganic chemicals such as hydrochloric acids, sulphuric acids, and sodium hydroxide, as well as organic solvents such as benzene methanol, acetone, and EDTA, can be used to regenerate the solvent. Other solvent regeneration technologies, such as microwave regeneration

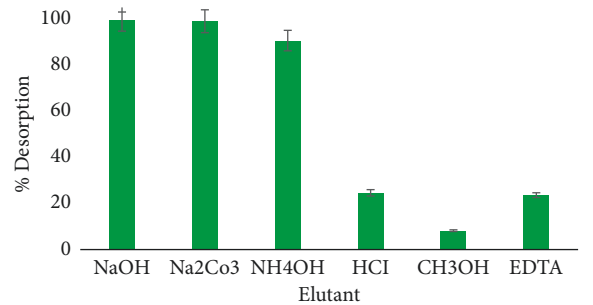


Figure 8: Desorption efficiency of RO16 from biochar for different solvents.

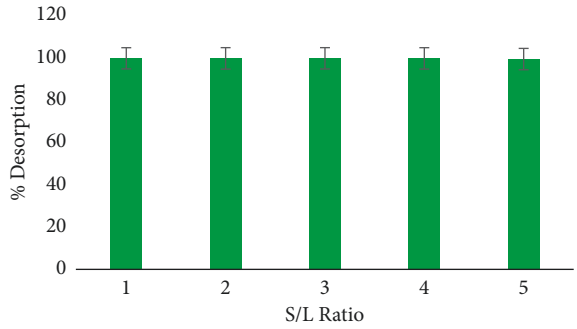


Figure 9: Desorption efficiency of RO16 for varying solid-to-liquid ratio.

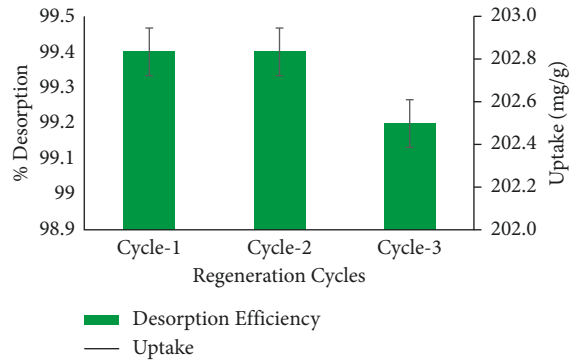


Figure 10: Desorption efficiency of RO16 for varying regeneration cycles.

and supercritical fluid regeneration, have recently been used [24]. Solvent regeneration methods for organic and inorganic solvents were used in this investigation. Figure 8 depicts the effect of various solvents on biochar and dye molecule desorption. Sodium hydroxide had the highest desorption efficiency of 99.8%, whereas sodium carbonate had the lowest desorption efficiency of 98.6%. Other solvents had a significantly lower desorption efficiency. Hydrochloric acid, for example, has a desorption efficiency of only 24.6%. The results of desorption demonstrated that desorption is the polar opposite of adsorption. At a pH value of 2, where more hydrogen ions are present, maximum adsorption was achieved, and desorption was very low in the hydrochloric acid solvent. Desorption efficiency was the highest with sodium hydroxide, which had very few hydrogen ions.

Desorption tests produce a large amount of solvent in which all hazardous contaminants are extracted from the sorbent and dissolved in it. The environmental disposal of these poisonous solvents becomes a serious challenge. As a result, determining the optimum volume of solvent necessary for the removal of harmful contaminants from the adsorbent has become a requirement. As a result, the solid-liquid (S/L) ratio was calculated to establish the optimal solvent volume. For example, an S/L ratio of 1 implies that the adsorption process used 100 ml of solute and the desorption process used 100 ml of liquid. Desorption efficiency is shown in Figure 9 for various S/L ratios. For S/L ratios of 1, 2, 3, 4, and 5, the solvent volume employed is 100, 50, 33.33, 25, and 20 ml, respectively.

Batch adsorption and desorption tests were carried out in the future. Figure 10 depicts the spent biochar's sorption and desorption efficiency. It has been discovered that biochar has the ability to regenerate three times. For example, the biochar's absorption capacity in the first, second, and third cycles was measured at 213.21, 213.21, and 212.78 mg/g, respectively, with a desorption efficiency of better than 98.8%. As a result, biochar made from *Ulva prolifera* has a lot of potential in terms of dye adsorption and desorption.

4. Conclusion

Biochar made from *Ulva prolifera* demonstrated to be an effective sorbent for removing reactive orange 16. The greatest removal efficiency was 85.8%, and the sorption capacity was 214.5 mg/g. The operating parameters were kept at a pH of 2, biochar dose of 2 g/L, temperature of 30 °C, and starting RO16 concentration of 500 mg/L. The Hill isotherm model suggested that a maximum sorption capacity of 252.36 mg/g could be achieved, with a good fit of 0.9729. A pseudo-second-order kinetic model with a decent fit of 0.9971 was used to track the adsorption mechanism. Increases in biochar dose and temperature increased removal efficiency, whereas increases in solution pH and beginning RO16 concentration decreased it. The characterization of biochar demonstrated that a large surface area of the sorbent will result in a good dye molecule sorption, and that the composition of the biochar was heterogeneous, allowing it to favour any type of dye molecule. According to thermodynamic experiments, the reactions are endothermic and spontaneous. According to desorption tests, sodium hydroxide is the best solvent, with a S/L ratio of 5, and three regeneration cycles may be successfully completed. Biochar made from *Ulva prolifera* offered various advantages, including availability, low-cost, ease of production, improved sorption capacity, and reusability. As a result, it was determined that biochar made from *Ulva prolifera* can be tested for various types of harmful contaminants in the future.

Data Availability

The data utilised to back up the study's findings are supplied in the article.

Disclosure

This research was carried out as part of the Samara University's employment in Ethiopia.

Conflicts of Interest

The authors declare that they have no conflicts of interest.

Acknowledgments

The authors are grateful for the help they received from Samara University in Ethiopia and the GMR Institute of Technology for completing this study.

References

[1] S. Waheed and C. M. Ashraf, "Synthesis and studies of some acid dyes," *Journal of the Chemical Society of Pakistan*, vol. 22, no. 1, pp. 49–54, 2000.

[2] J. Kanagaraj, T. Senthilvelan, R. Panda, Kavitha, and S. Kavitha, "Eco-friendly waste management strategies for greener environment towards sustainable development in leather industry: a comprehensive review," *Journal of Cleaner Production*, vol. 89, pp. 1–17, 2015.

[3] T. Robinson, G. McMullan, R. Marchant, and P. Nigam, "Remediation of dyes in textile effluent: a critical review on current treatment technologies with a proposed alternative," *Bioresource Technology*, vol. 77, no. 3, pp. 247–255, 2001.

[4] J. Rovira and J. L. Domingo, "Human health risks due to exposure to inorganic and organic chemicals from textiles: a review," *Environmental Research*, vol. 168, pp. 62–69, 2019.

[5] E. Soto Cantu, "Modern developments in the spray-drying industries," *Recent Patents on Materials Science*, vol. 4, no. 2, pp. 106–121, 2011.

[6] S. Atalay, Ersoz, and G. Ersöz, "Advanced oxidation processes for removal of dyes from aqueous media," in *Green Chemistry for Dyes Removal from Waste Water: Research Trends and Applications*, S. K. Sharma, Ed., Wiley, New Jersey, USA, pp. 83–117, 2015.

[7] M. O. A. Mäkinen and T. J. Jääskeläinen, "Improving optical properties of printing papers with dyes: a theoretical study," *Nordic Pulp and Paper Research Journal*, vol. 22, no. 2, pp. 236–243, 2007.

[8] M. Kucharska and J. Grabka, "A review of chromatographic methods for determination of synthetic food dyes," *Talanta*, vol. 80, no. 3, pp. 1045–1051, 2010.

[9] S. Kobylewski and M. F. Jacobson, "Toxicology of food dyes," *"International Journal of Occupational and Environmental Health*, vol. 18, no. 3, pp. 220–246, 2012.

[10] S. O. Obare, C. De, W. Guo et al., "Fluorescent chemosensors for toxic organophosphorus pesticides: a review," *Sensors*, vol. 10, no. 7, pp. 7018–7043, 2010.

[11] E. Mariani, C. Neuhoff, and C. Villa, "Preliminary COMMUNICATION: application of high-performance liquid chromatography in the analysis of direct dyes in semipermanent hair colouring cosmetics," *International Journal of Cosmetic Science*, vol. 19, no. 2, pp. 51–63, 1997.

[12] R. Gokulan, P. Ganapathy Ganesh, and J. Jegan, "Remediation of complex remazol effluent usingbiochar derived from green seaweed biomass," *International Journal of Phytoremediation*, vol. 21, no. 12, pp. 1179–1189, 2019.

[13] S. N. H. Jaafar, L. J. Minggu, K. Arifin, M. B. Kassim, and Wan, "WRD 2017, 'Natural dyes as TiO_2 sensitizers with membranes for photoelectron chemical water splitting: an overview," *Renewable and Sustainable Energy Reviews*, vol. 78, pp. 698–709, 2017.

[14] R. Ziessel, G. Ulrich, A. Haefele, and A. Harriman, "An artificial light-harvesting array constructed from multiple bodipy dyes," *Journal of the American Chemical Society*, vol. 135, no. 30, pp. 11330–11344, 2013.

[15] I. M. Banat, P. Nigam, D. Singh, and R. Marchant, "Microbial decolorization of textile-dye containing effluents: a review," *Bioresource Technology*, vol. 58, no. 3, pp. 217–227, 1996.

[16] A. Baban, A. Yediler, and N. K. Ciliz, "'Integrated water management and CP implementation for wool and textile blend processes," *Clean - Soil, Air, Water*, vol. 38, no. 1, pp. 84–90, 2010.

[17] C. Zaharia, D. Suteu, A. Muresan, R. Muresan, and A. Popescu, "Textile wastewater treatment by homogenous oxidation with hydrogen peroxide," *Environmental Engineering and Management Journal*, vol. 8, no. 6, pp. 1359–1369, 2009.

[18] M. A. M. Salleh, D. K. Mahmoud, W. A. W. A. Karim, and A. Idris, "Cationic and anionic dye adsorption by agricultural solid wastes: a comprehensive review," *Desalination*, vol. 280, no. 1-3, pp. 1–13, 2011.

[19] T. Estlander, "Allergic dermatoses and respiratory diseases from reactive dyes," *Contact Dermatitis*, vol. 18, no. 5, pp. 290–297, 1988.

[20] K. L. Hatch and H. I. Maibach, "Textile dye dermatitis," *Journal of the American Academy of Dermatology*, vol. 32, no. 4, pp. 631–639, 1995.

[21] Sm. Wilkinson and K. McGechaen, "'Occupational allergic contact dermatitis from reactive dyes," *Contact Dermatitis*, vol. 35, no. 6, pp. 376–378, 1996.

[22] K. Thoren, B. Meding, R. Nordlinder, and L. Belin, "Contact dermatitis and asthma from reactive dyes," *Contact Dermatitis*, vol. 15, no. 3, p. 186, 1986.

[23] P. Saha, S. Chowdhury, and M. Tadashi, Eds., *Insight into Adsorption Thermodynamic*, pp. 349–364, IntechOpen, London, UK, 2011, Chapter 16.

[24] Y. Morikawa, K. Shiomi, Y. Ishihara, and N. Matsuura, "Triple primary cancers involving kidney, urinary bladder, and liver in a dye worker," *American Journal of Industrial Medicine*, vol. 31, no. 1, pp. 44–49, 1997.